Effect of parameter uncertainty on water quality predictions in distribution systems-case study

M. F. K. Pasha and K. Lansey

ABSTRACT

The effect of parameter uncertainty on water quality in a distribution system under steady and unsteady conditions is analyzed using Monte Carlo simulation (MCS). Sources of uncertainties for water quality include decay coefficients, pipe diameter and roughness, and nodal spatial and temporal demands. Results from the system analyzed suggest that water quality estimates are robust to individual parameter estimates but the total effect of multiple parameters can be important. The largest uncertainties occur when flow patterns are altered. The study also provides guidance on difficulties in model calibration. For example, the wall decay had the largest influence on model prediction for the system that was reviewed and is one of the most difficult to measure given its variability between pipes.

Key words | Monte Carlo simulation, uncertainty analysis, water distribution systems, water quality

M. F. K. Pasha
K. Lansey (corresponding author)
Department of Civil Engineering and Engineering Mechanics,
University of Arizona,
Tucson AZ 85721,
USA
Tel.: +1 520 621 2512
Fax: +1 520 621 2550
E-mail: *lansey@engr.arizona.edu*

INTRODUCTION

Since the passage of the Safe Drinking Water Act (http://www.epa.gov/safewater/regs.html) in 1990, researchers have been motivated to work on water quality and system hydraulics issues in water distribution system design and operation. Before 1990 water quality requirements were only imposed at the water source: thus, the primary concern of the water distribution system was systems hydraulics. Today, maintaining disinfection and pressure levels are equally important.

Water distribution system modeling can be used as a basis of planning and operational decisions. However, model accuracy and uncertainty impact model-based decisions. Uncertainty is a characteristic that results from the lack of perfect information of a system. It can be quantified in different ways. Following the textbook engineering definition (Tung & Yen 2005), the standard deviation and variance are used to quantify uncertainty in this study. Model prediction uncertainty results from uncertainties in model parameters that are determined through calibration or are based upon modeler judgment. However, field data to calibrate some model parameters is inherently uncertain due to measurement error, and is expensive, difficult and sometimes impossible to collect. For example, although bulk decay coefficients are easy to measure, pipe wall decay coefficients cannot be measured directly and may vary from pipe to pipe. Similarly, demand variability over time and space is almost impossible to measure. Likely, pipe-related parameters such as diameter and roughness coefficient are the easiest to estimate using pressure data.

Uncertainty in pressure head due to pipe roughness and nodal demands has been evaluated from the perspective of system reliability (Bao & Mays 1990; Xu & Goulter 1998). However, water quality uncertainty analysis within a distribution system has been studied little. Water quality within the distribution systems is strongly affected by water quality model parameters, such as bulk and wall decay coefficients. In addition, since transport is dominated by advection, hydraulic parameters and conditions also impact water quality. This is most clearly seen in the effects of tanks due to flows to and from the storage facility. The hydraulic

doi: 10.2166/hydro.2010.053

system representation also affects the flow distribution and travel times within the system. Many modelers suggest that all pipe models are required to adequately represent the true flow patterns. As more pipes are introduced, more uncertain parameters must be defined or calibrated for those components.

This paper examines the impact of alternative sources of uncertainty on water quality predictions by examining both steady and unsteady conditions for two relatively large systems. The objective is to study the effect of alternative uncertain parameters sets on uncertainty levels of water quality variables through Monte Carlo simulation (MCS). The evaluated input parameters are the decay coefficients, pipe roughnesses, pipe diameters and nodal demands. Spatial and temporal nodal demand variabilities are also considered. The model output of interest is the nodal concentrations throughout the system. Evaluating the MCS results provides insights into the relative importance of the different model parameters and potential implications on model calibration and use.

The relative impact of uncertain parameters changes with system conditions. For example, water is often stored in the tank to provide adequate pressure and for emergency use at the expense of water quality deterioration. Thus, the uncertainty in delivered water as related to the amount of emergency storage is examined. Similarly, daily demand patterns change between seasons and the relative impact will vary.

BACKGROUND

Uncertainty analysis has been applied to water distribution systems in attempts to quantify system reliability. Wagner *et al.* (1988) performed MCS for general systems. However, they only considered pipe breaks and pump outages as the random phenomena and found their effects on nodal pressure heads. Bao & Mays (1990) defined hydraulic reliability as the water distribution system performance measure and mechanical reliability as the ability of the system components to provide continuing and long-term operation without frequent repairs. Based on those definitions, they completed an MCS study considering uncertainties of future demand, pressure head and pipe roughness and examined the impact of uncertainties on nodal reliability.

Xu & Goulter (1998) considered uncertainties in nodal demands, pipe roughness and reservoir/tank levels and observed their impacts on nodal pressure heads. A first-order Taylor series expansion to the nonlinear hydraulic model was applied to develop the linearized model and verified by MCS.

Sadiq *et al.* (2004) presented a risk analysis associated with water quality in the distribution systems. However, the authors computed the risk based on the external sources that can deteriorate the water quality in the systems. The sources included to compute the risks were: intrusion of contaminants into the system (through connection) or permeation of organic compounds through plastic components, re-growth of bacteria in the systems including pipe and storage facilities, water treatment breakthrough, leaching of chemicals and the corrosion of systems components. The system parameters that are involved in deteriorating in-system water quality were not included in their study. Barkdoll & Didigam (2004) evaluated the impact of uncertain demands on pressure and water quality. They limited their study to two relatively small networks for steady and unsteady conditions. Only an average demand was considered as uncertain and fluctuations in the daily temporal demand factors were not considered.

Pasha & Lansey (2005) conducted MCS under steady conditions considering pipe diameter and roughness decay coefficients, and nodal demands as sources of uncertainty. However their analysis did not include unsteady conditions.

Khanal *et al.* (2006) conducted a two-part contamination level investigation into the distribution systems. In part I, the zone of influence was mapped based on calculated exposure index and in part II the Latin hypercube sampling technique was used to perform a generalized sensitivity analysis to find out network response to base demand, storage capacity, injection mass and injection duration. They concluded that in some cases storage capacity is important while the injection duration is the least important. Other important parameters such as pipe diameter and roughness, bulk and wall decay coefficients were not considered in their study.

Given the range of information required to compute water quality, all parameters should be considered and the

relative impact of each parameter on the model output should be evaluated. With this information, modelers can begin to assess what data should be collected and the importance of acquiring data to make good parameter estimates. Thus, a water quality model can be calibrated efficiently with the amount and quality of data collected. MCS consists of successive evaluations of the equations describing the system for alternative realizations of the system parameters. The following sections summarize the hydraulic and water quality relationships to show how the parameters fit within the model.

Systems equations

Water distribution network hydraulics are described by conservation of mass and energy and water quality is based upon conservation of mass at a node and advective transport in a pipe.

Hydraulics relationships

Several formulations of conservation of mass and energy can be written for a water distribution system under steady conditions (Boulos *et al.* 2004). Here the pipe equation formulation is summarized. For a junction that connects two or more pipes, conservation of mass is written as

$$\sum_{l\in J_{\text{in},i}} Q_l - \sum_{l\in J_{\text{out},i}} Q_l = q_i \tag{1}$$

where Q_I are the pipe flows, q_i is the external demand or supply, and $J_{\text{in},i}$ and $J_{\text{out},i}$ are the set of pipes supplying and carrying flow from node i, respectively.

For pipe l that connects nodes A and B, conservation of energy is

$$H_A - H_B = h_{L,l} \tag{2}$$

where H_A and H_B are the total energy at nodes A and B, respectively, and $h_{L,l}$ is the head loss in connecting pipe l. The head loss can be estimated by a number of equations including the Darcy–Weisbach and Hazen–Williams equations. Each equation and its associated parameters can be modeled in an MCS. The empirical Hazen–Williams equation is most widely used in the USA for water distribution system analysis:

$$h_L = K_u(Q/C_{\text{HW}})^{1.852}(L/D^{4.87}). \tag{3}$$

where K_u is a unit constant, and D, L, Q and C_{HW} are the diameter, length, flow and Hazen–Williams roughness coefficient of the pipe respectively. EPANET (Rossman 2002) iteratively solves this set of nonlinear equations with a Newton's type method for the unknown H's and Q's given all pipe diameters, lengths and roughness coefficients and all nodal demands, following Todini & Pilati (1988).

Unsteady hydraulic conditions are represented by introducing a tank to the system with a water surface level that varies with flows to and from the tank. Nodal demands are assumed to vary through the analysis period in a series of discrete time steps.

Water quality relationships

Four mechanisms are involved with fluid and constituent transport: advection, molecular and turbulent diffusion, and dispersion. Turbulent diffusion does not affect longitudinal transport and so is unimportant here. In most available models, dispersion is neglected since the flow velocities are normally high, resulting in uniform velocity distributions. Molecular diffusion is very small compared to other transport mechanisms so it is also neglected (Boulos *et al.* 2004). Therefore, advection transport at the flow velocity is the only transport mechanism considered. In this case, conservation of constituent mass for a pipe can be written in differential form as

$$\partial C/\partial t + V\partial C/\partial x = r(C) \tag{4}$$

where V is the flow velocity that is determined by solving the hydraulic equations. $\partial C/\partial x$ is the rate of change in concentrations between the inflow and outflow sections of a differential element, $\partial C/\partial t$ is the rate of change of constituent concentration within the differential element and $r(C)$ is the reaction relationship. The general form of $r(C)$ for a decay process is

$$r(C) = k(C - C^*)C^{nc-1} \tag{5}$$

where C^* is the limiting concentration, k is the reaction constant and nc is the reaction order. Chlorine, which can

decay completely ($C^* = 0$), is modeled by a first-order reaction ($nc = 1$) in this application, so $r(C) = kC$. Any reaction order can be evaluated using MCS.

Decay reactions occur in the water with reacting substances present in the water and with materials on the pipe wall. As a result, the reaction constant k is the sum of two coefficients, the bulk reaction coefficient, k_b, and the wall reaction coefficient, k_{wall} or

$$k = k_b + k_{\text{wall}}. \tag{6}$$

Rossman *et al.* (1994) reported that pipe wall coefficients are affected by three factors: the reactive ability of biofilm layer, the available wall area for reactions and the movement of water to the wall. The reactive nature of the wall material is measured by another coefficient, the global wall reaction rate, k_w. For first-order reaction the wall decay coefficient k_{wall} can be written as (Rossman *et al.* 1994)

$$k_{\text{wall}} = 2k_w k_f / R(\text{abs}(k_w) + k_f) \tag{7}$$

where k_f is a mass transfer coefficient that is a function of the turbulence in the pipe that is related to the Reynolds number, R is the pipe radius and abs is the absolute value operator. The transport Equations (Equations (4)–(7)) can be solved by several methods. EPANET (Rossman 2002) uses the time-driven method.

The above Equations (1)–(7) show that the parameters–nodal demand, pipe diameter, pipe roughness and bulk and wall reaction coefficients–all directly affect the nodal constituent levels. Reaction coefficients appear within the reaction relationship but wall decay is influenced by the degree of turbulence that is related to hydraulic conditions (Rossman 2002). Thus, the hydraulic parameters (C_{HW}, D and q) indirectly affect constituent decay as well as directly control flow velocities that dominate constituent transport.

All five parameters were considered as uncertain in this analysis. A pipe's effective diameter reduces over time because of encrusted materials on the pipe walls. Pipe roughness also increases due to the encrusted materials. Thus, these two parameters are uncertain. The bulk decay coefficient is related to many factors, including temperature and pH, that may vary over time. The wall decay coefficient is very difficult to measure accurately since it depends on the reactive ability of the biofilm layer, the wall area available for reactions and the movement of water. Thus, these two decay coefficients are also uncertain. Demands are inherently uncertain due to random water consumption.

METHODOLOGY

MCS for water distribution quality analysis consists of five steps. The first step is to generate sets of random numbers for each parameter set. Defining parameters' values based on the random numbers and parameter probability distributions is the second step. Next, hydraulic and water quality simulations are completed using EPANET (Rossman 2002). Finally, statistics of disinfectant levels are computed for nodes of interest. These steps are repeated until the statistics of the output converge to consistent values (Step 5).

Generating random parameters (Steps 1 and 2)

For each realization, a set of random numbers are generated in the range 0–1. The number of random values equals the number of uncertain parameters. The parameter values are then computed based upon their assumed distributions. For a uniform distribution, the parameter, P_{uniform}, is found by

$$P_{\text{uniform}} = \text{rnd}(P_{\text{ul}} - P_{\text{ll}}) + P_{\text{ll}} \tag{8}$$

where P_{ul} and P_{ll} are the upper and lower bound of the parameter and rnd is the generated random number. Normally distributed parameters values are determined by

$$P_{\text{normal new}} = \mu + \sigma^* Z \tag{9}$$

where μ and σ are the mean and standard deviation of the parameter and Z is the standard normal deviate that is found using the following approximation (Abramowitz & Stegun 1972)

$$Z = t - (a_0 + a_1 t)/(1 + b_1 t + b_2 t^2). \tag{10}$$

where $a_0 = 2.30753$; $a_1 = 0.27061$; $b_1 = 0.99229$ and $b_2 = 0.04481$. t is found from the random number by

$$t = (\ln(1/\text{rnd}^2)^{1/2} \quad \text{where } 0 < \text{rnd} < 0.5. \tag{11}$$

If the generated rnd is greater than 0.5, then rnd = 1-rnd and the resulting sign of Z is changed from positive to negative.

Computing model variable statistics (Steps 3–5)

As noted earlier, EPANET is used to compute the pressure head and water quality for each realization of random input. The link between the random parameter generation and EPANET is completed using the EPANET Toolkit (Rossman 2002), which is also used to extract the model results. The mean and standard deviation of the output variables are computed as the MCS progresses. The process is repeated for a defined number of realizations or until the output statistics, i.e. mean and standard deviation of chlorine concentrations, converge to consistent values.

Analyses were completed for steady and unsteady conditions. Cyclical steady conditions were evaluated in the unsteady analysis. Experiments were completed by varying individual parameters, all parameters simultaneously, and all parameters omitting one.

APPLICATION NETWORK: EXAMPLE 1

Steady conditions

The first network that is analyzed in this study is network NET2A from the EPANET User's Manual (Rossman 2002) (Figure 1) that consists of 35 pipes, 30 nodes, one reservoir (node 32) and one source (node 31). For the steady state analysis, demands, the reservoir and source levels, and source concentration were held constant. Although network hydraulics are assumed to reach steady conditions nearly instantaneously, water quality requires time to reach a steady condition. A 72 h hydraulic and water quality analyses were completed. The hydraulic time step, quality time step and pattern time step were 1:00, 0:05 and 1:00 h, respectively.

Chlorine is the disinfectant of interest. It was assumed to decay by following a first-order reaction with $k_b = -0.3$ 1/d and $k_w = -0.3$ 1/d. The input concentrations generated at source and reservoir were assumed to be 1.0 mg/l and 0.5 mg/l, respectively. All pipe and base demand data were taken directly from the EPANET manual. Pipes downstream of node 26 were dominated by laminar flow, which violates the assumption in the defined water quality model, so downstream pipes were truncated and demands were lumped at node 26.

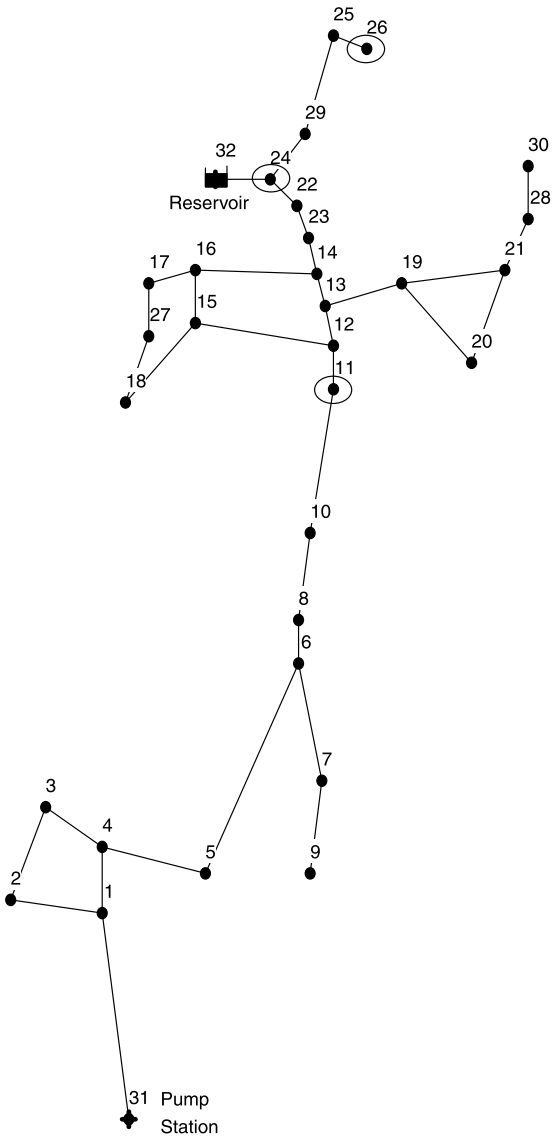

Figure 1 | Water distribution network NET2A (Example 1 network) for steady case. For the unsteady case, the reservoir is changed to a tank and three pumps are introduced at the source (pump station).

Due to a lack of literature, bulk decay and wall decay coefficients were assumed to follow normal distribution the roughness and nodal demands were assumed to follow truncated normal distribution. The coefficient of variation used for all of these parameters is 0.1. Pipe roughness values were limited to 25 units above or below the mean or a maximum and minimum of 140 and 80, respectively. A check is completed to ensure the set of generated C_{HW} values are within their bounds. If not, the value is discarded and a new random number is generated.

Pipe diameters are assumed to follow uniform distributions with a range from the nominal diameter of 12.7 mm (0.5 inches). However, log-normal distribution can be an alternative. The range in which a diameter can vary is small (12.7 mm).

To ensure that the generated demands do not vary significantly from the system's mean demands the total generated demand must not change the total mean demand by more than 5%. If they do, the set of generated demands is rejected and a new set of demands is generated. Rejection of the generated demands occurred very rarely. Table 1 summarizes the statistics used for the set of MCS runs.

The nodal concentrations were examined at three locations in the system (nodes, 11, 24 and 26 (Figure 1)) at hour 72. The three locations are intended to examine the effects of travel time from the source. At hour 72, the average water ages for nodes 11, 24 and 26 were 4.2, 7.4 and 11.5 h, respectively. These values are close to the travel times to those locations. The longer simulation period (72 h) was used to ensure steady water quality conditions were found for all locations and generated parameter sets. It was observed that MCS statistics converge relatively quickly (between 3,000–5,000 realizations). However, to ensure convergence 10,000 realizations were conducted in each experiment (Figure 2).

To understand the impact of each parameter's uncertainty a set of experiments was completed with only one parameter being uncertain and all others constant. An MCS is unnecessary for the decay coefficients as they are single values but for ease of programming they were completed. Results for these experiments are shown as box and whisker plots (Figure 3(a)). The effect of each parameter can be assessed from the relative length of the box and whisker. The combined effect of a parameter set was then assessed in a set of five experiments by fixing one parameter per experiment, allowing all others to be uncertain and completing an MCS (Figure 3(b)).

The variance of a function of several parameters (e.g. a and b) can be approximated by

$$\mathrm{Var}(f(a,b)) = (\partial f/\partial a)^2\mathrm{Var}(a) + (\partial f/\partial b)^2\mathrm{Var}(b) + 2(\partial f/\partial a)(\partial f/\partial b)\mathrm{Cov}(a,b) + O(n^{3/2}). \quad (12)$$

where $\mathrm{Var}(f(a,b))$ is the total function variance due to parameters a and b. The first and second terms on the RHS are the contributions of parameters a and b, independently. The third term is the component from the dependence between a and b and the fourth term is noise or model uncertainty. In this study parameters were assumed to be independent; thus the covariance term is zero. Also, the model is assumed to be known exactly.

Results

As seen in Figures 3(a, b), the global wall decay coefficient has the most effect on concentrations at node 11. The box length is the largest when only one parameter, the global wall decay coefficient, was considered uncertain (Figure 3(a)). Similarly, the box length is the smallest when it was considered as certain (Figure 3(b)). Node 11 is reasonably close to the pump station and therefore the travel time to that node is relatively short. The result of the short travel time is that bulk decay has little influence while the global wall decay has the highest impact of all parameters. If flow is steady, the total uncertainty at a

Table 1 | Statistics for uncertain parameters (both Example networks)

	Pipe diameter D	Pipe roughness C	Base demand q	Demand factor q_f	Bulk decay coefficient k_b	Wall decay coefficient k_w
Mean	Varies*	Varies*	Varies*	Varies*	−0.3 (1/d)	−0.3 (1/d)
Standard deviation or range	0.5″	Varies*	Varies*	Varies*	0.03	0.03
Coefficient of variation	–	0.1	0.1	0.1	0.1	0.1
Probability distribution	Uniform	Truncated normal	Truncated normal	Normal	Normal	Normal

*'Varies' in first row of Table 1 means each pipe and node has its own mean parameter value (e.g. diameter, roughness and demand). Since standard deviations are calculated from means using coefficients of variation they also vary pipe to pipe and node to node. However, single mean values have been used for wall and bulk decay coefficients for the whole network.

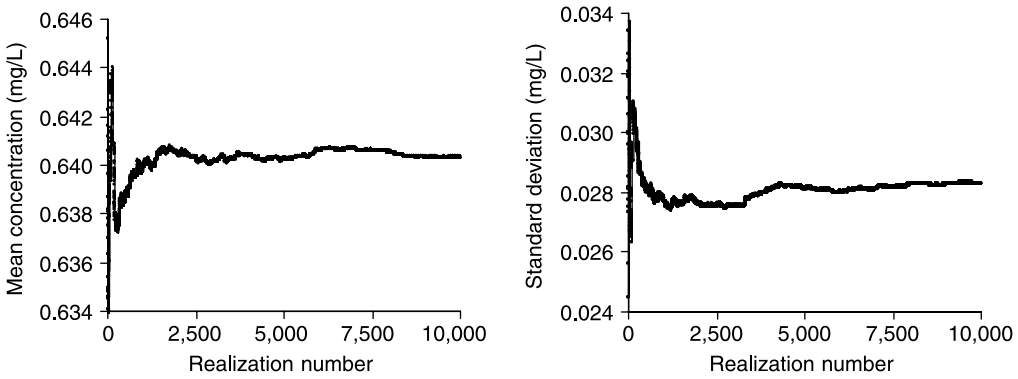

Figure 2 | Mean and standard deviation of concentration at different realizations considering all parameters uncertain at node 24 (Example 1 network).

particular location based on Equation (12) is approximately equal to the sum of the uncertainties due to each parameter considered separately. Therefore, the output variance is highest when all parameters are uncertain. This observation was confirmed in Figures 3(a, b). The standard deviation at node 11, $s_{11} = 0.014$ mg/l. and coefficient of variation at node 11, $CV_{11} = 0.019$, when all parameters are uncertain.

Node 24 is located in the middle of the system and receives a mixture of flows from the source and the tank. The global wall decay coefficient and demand make the largest contributions to the node's uncertainty (Figure 3(a)). The magnitude of the water quality uncertainty due to the global wall decay coefficient and demand is higher at this location compared to nodes 11 and 26 (Figure 3(a)). As a result of a longer travel distance, decay due to wall interactions is larger than node 11. Thus, water quality is more sensitive to the global wall decay coefficient. Demand changes alter the flow pattern and the source of water passing through this node. Since the chlorine concentrations of water from the source after decay are much less than the water from the nearby reservoir, this causes higher uncertainty in the concentrations at node 24. Similar to node 11, pipe diameter and roughness and bulk decay have little influence on the water quality at this node (Figures 3(a, b)).

Node 26 is in the distant portion of the system and has a higher water age and lower chlorine concentrations (mean concentration $= 0.51$ mg/l). This node is influenced by all input parameters to a larger degree. The global wall decay coefficient and discharge have the largest influence due to longer travel times. Compared to nodes 11 and 24, bulk decay and pipe diameter and roughness are more important at this node (Figure 3(a)). However, pipe diameter and roughness have the smallest influence relative to other input parameters at node 26. The standard deviation for node 26's concentration is about 0.027 mg/l when all uncertain parameters are considered (Figure 3(b)) but, more significantly, the coefficient of variation is 0.053 since the concentration is low. In the upper portion of this system, the pipe velocities are smaller and thus the decay in the path to node 26 is dominated by bulk reactions as seen in Figure 3(a).

To observe the importance of parameters, Pearson product-moment correlation coefficient (PCC) and Spearman's rank correlation coefficient (RCC) (Tung & Yen 2005) were calculated at steady conditions from the MCS samples for several nodes (Table 2). Based on the magnitude of the terms, water quality estimates are more sensitive to water quality parameters (decay coefficients) than hydraulic parameters (diameter, roughness and demand). For nodes with relatively short travel times (12, 15 and 22) the wall coefficient had the largest RCC. On the other hand, for nodes 25 and 27 the RCC for the bulk decay was highest due to the long travel times and low velocities in pipes off the main trunkline.

Finally, the ratio of the Spearman to Pearson coefficients provides an indication of the nonlinearity over the range of the input parameter that is a better indicator compared to a single-point sensitivity term. A larger value implies higher nonlinearity. It is interesting to note that the decay parameters, although being the most sensitive, are the most linear while the parameters causing less uncertainty have a more non linear effect.

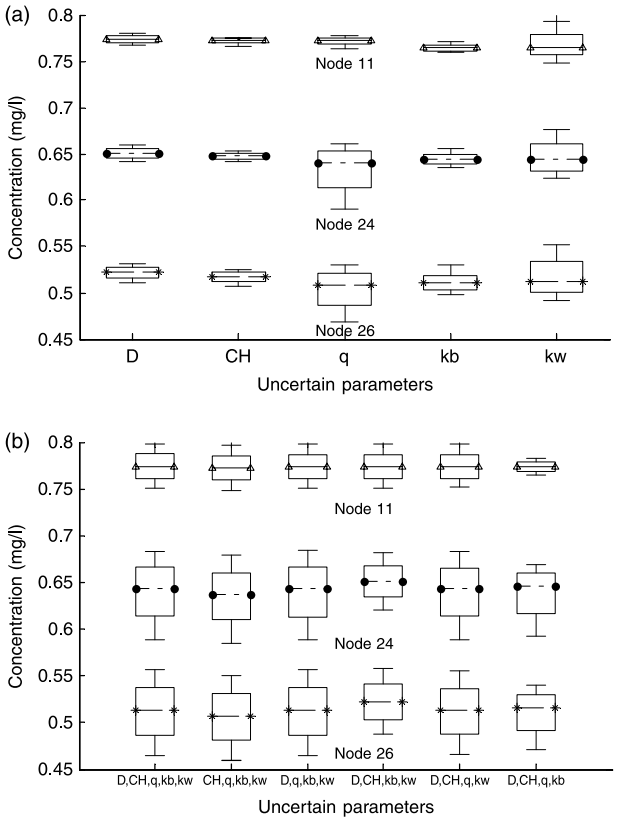

Figure 3 | (a) Box and whisker diagrams for MCS results under steady conditions for individual parameter uncertainty (Example 1 network). (b) Box and whisker diagrams for MCS results under steady conditions for multiple uncertain parameters (Example 1 network). Box and whisker diagram for concentration at different nodes showing median, 1st and 3rd quartiles, and 5th and 95th percentiles for different sets of uncertain parameters (*D* = pipe diameter, *CH* = pipe roughness, *q* = nodal demand, *kb* = global bulk decay coefficient and *kw* = global wall decay coefficient).

Unsteady conditions

To examine the effect of temporal flow conditions, the Net2A system was modeled in an extended period analysis (EPS). As shown in Figure 1, the reservoir was changed to a tank. Three identical pumps at the source were represented with the design point option with Q_{design} and H_{design} equal to 31.8 m^3/h (8.83 l/s) and 85.3 m, respectively. Pumps were operated using a control policy based on the tank level containing three rules: less than 3.1 m of water in the tank turn on all three pumps, exceed 4.57 m level turn off one pump and exceed 7.62 m level turn off all pumps.

The source water level and its concentration were held constant at 0 m and 1 mg/l, respectively. The 24 h average demand pattern listed in Table 3 was repeated for a 480 h simulation period. A cyclical steady state quality and quantity pattern was reached before 480 h but extra time was added to allow for uncertainty in changing parameters. The same hydraulic time step, quality time step and pattern time step were also used in the EPS as in the steady state analysis. The same decay coefficients were used as in the steady state analysis. Nodal concentrations were examined at three locations in the system (nodes 11, 24 and 26) from hours 456 to 480 (12 am to 12 am). MCS runs were completed (1) varying one parameter with others remaining fixed and (2) considering all parameters uncertain together. The MCS was terminated if the change of standard deviation of concentration did not exceed 0.0001 mg/l between 250 realization increments or 10,000 realizations were evaluated.

For unsteady conditions the total system demand factor (q) is generated as in the steady case and applied to the average demand for each node to generate the base demand over a day for that particular node. Since each node's demand varies over time, a second temporal demand factor (q_f) is generated for each node for each time period. This temporal demand factor introduces uncertainty about the average nodal demand as a function of time. The final nodal demand at node j and time t, $q_{t,j}$, is computed by

$$q_{t,j} = q^f_{t,j} q^n_j DF_t qb_j \tag{13}$$

where qb_j is the base demand for node j, DF_t is the deterministic base demand multiplier for time t, q^n_j is the random nodal demand factor for node j and $q^f_{t,j}$ is the random temporal demand factor for time t and node j. In the MCS, uncertainties were introduced for $q^f_{t,j}$ as an independent parameter and the total demand uncertainty, q^n_j. Both of these demand factors were assumed to follow the normal distribution. Since no information is available on potential relationships, all parameters are assumed to be uncorrelated.

According to Equation (12) it is observed in the steady case that prediction uncertainty when all the parameters were considered uncertain is higher than the uncertainty due to any parameters considered separately. However, in the unsteady case changes in the flow pattern and system operations play an important role. It is observed that, due to change in the flow pattern, there are discrete changes in

Table 2 | Pearson and Spearman rank correlation coefficients and their divisor for different uncertain parameters for nodes (Example 1 network)

		Pearson correlation coefficients (PCC)			Spearman rank correlation coefficients (RCC)			Divisor (RCC/ PCC)		
Node	Parameter	Mean	Min	Max	Mean	Min	Max	Mean	Min	Max
12	Diameter	0.04	0.00	0.22	0.01	0.00	0.02	1.51	0.01	14.86
	Roughness	0.02	0.00	0.30	0.01	0.00	0.02	3.24	0.00	43.40
	Demand	0.05	0.00	0.27	0.01	0.00	0.02	0.95	0.02	7.18
	Bulk Coef.	0.72	0.72	0.72	0.17	0.17	0.17	0.24	0.24	0.24
	Wall Coef.	0.95	0.95	0.95	0.30	0.30	0.30	0.31	0.31	0.31
15	Diameter	0.04	0.00	0.27	0.01	0.00	0.03	1.24	0.00	9.66
	Roughness	0.03	0.00	0.21	0.01	0.00	0.03	1.07	0.03	8.82
	Demand	0.05	0.00	0.29	0.01	0.00	0.02	1.01	0.01	13.77
	Bulk Coef.	0.81	0.81	0.81	0.02	0.02	0.02	0.02	0.02	0.02
	Wall Coef.	0.98	0.98	0.98	0.18	0.18	0.18	0.19	0.19	0.19
22	Diameter	0.04	0.00	0.39	0.01	0.00	0.03	6.17	0.00	162.36
	Roughness	0.04	0.00	0.57	0.01	0.00	0.03	1.27	0.00	12.81
	Demand	0.06	0.00	0.73	0.01	0.00	0.02	13.14	0.01	211.44
	Bulk Coef.	0.85	0.85	0.85	0.01	0.01	0.01	0.01	0.01	0.01
	Wall Coef.	0.97	0.97	0.97	0.11	0.11	0.11	0.12	0.12	0.12
25	Diameter	0.04	0.00	0.22	0.01	0.00	0.02	1.23	0.01	8.07
	Roughness	0.02	0.00	0.17	0.01	0.00	0.03	5.42	0.00	123.30
	Demand	0.12	0.01	0.45	0.01	0.00	0.02	0.14	0.00	1.23
	Bulk Coef.	0.91	0.91	0.91	0.13	0.13	0.13	0.14	0.14	0.14
	Wall Coef.	0.97	0.97	0.97	0.09	0.09	0.09	0.09	0.09	0.09
27	Diameter	0.04	0.00	0.18	0.01	0.00	0.02	0.76	0.01	4.78
	Roughness	0.01	0.00	0.11	0.01	0.00	0.01	6.51	0.05	175.68
	Demand	0.12	0.01	0.45	0.01	0.00	0.02	0.14	0.00	0.83
	Bulk Coef.	0.88	0.88	0.88	0.09	0.09	0.09	0.10	0.10	0.10
	Wall Coef.	0.96	0.96	0.96	0.06	0.06	0.06	0.06	0.06	0.06

pump operations and flow. Thus, the gradients in Equation (12) are not continuous. As a result, the uncertainty due to all parameters can be seen to be less than the uncertainty due to individual parameters at a particular time.

Node 11

The average concentration over the 24 h cyclical demand period for node 11 is shown in Figure 4(a). The concentration at node 11 is highest during the early morning and gradually falls until mid-afternoon. Node 11's demand is always provided by flow from the pump station source. The velocities in the pipes located between the source and node 11 are lowest between 2 am and 3 pm. This water reaches node 11 from 3 am to 4 pm, resulting in the lower average concentrations compared to the remainder of the day due to the longer travel times. High concentrations during the remainder of the day are due to higher velocities and shorter travel times.

Standard deviations of chlorine concentration for different uncertain parameters are shown in Figures 4(b, c). The overall magnitude of uncertainty (Figure 4(c)) is small at this node except for around 4 pm. As noted, chlorine decay is closely related to travel time. In a constant diameter pipe, velocity increases directly with flow rate. Therefore, during high flow periods chlorine decay is low.

Table 3 | Temporal demand factors for different conditions (both Example networks)

Time	Temporal demand multipliers	Time	Temporal demand multipliers
12 am	0.5	12 pm	1.16
1 am	0.48	1 pm	1.17
2 am	0.45	2 pm	1.21
3 am	0.4	3 pm	1.23
4 am	0.46	4 pm	1.36
5 am	0.64	5 pm	1.57
6 am	0.85	6 pm	1.75
7 am	1.2	7 pm	1.5
8 am	1.37	8 pm	1.15
9 am	1.27	9 pm	0.85
10 am	1.16	10 pm	0.66
11 am	1.15	11 pm	0.58

On the other hand, if flows are small, decay is high. Around 2 am and 3 pm, the source pump operations generally changed. At 2 pm one of the three operating pumps is turned off and flow from the pump station decreases. This pump is turned back on at 3 pm and the pump station flow increases. These pump switches are reflected in the concentration changes at these time (Figure 4(a)). Small demand changes can cause the pump switching to occur slightly before or after the noted times, causing more variability in pumping rates and higher water quality uncertainty. The demand uncertainty contributions to overall chlorine concentration uncertainty are quite small during the remainder of the day.

With the exception of these two periods the global wall decay coefficient provides the largest contribution to node 11's concentration uncertainty. The uncertainty pattern due to bulk decay coefficient is similar to, but lower than, the global wall decay coefficient. In the turbulent flow in the pipes supplying node 11, the wall decay coefficient is larger and has more impact than the bulk decay coefficient.

Pipe diameter and roughness are the least significant parameters for this node. Although diameter changes cause velocity and water age differences, these changes are apparently less than that caused by demand uncertainty. Equation (12) can be used to estimate water quality variability. This relationship is in essence the first-order second moment variance estimate method based on a Taylor's series expansion and ignoring the higher-order terms. Calculations have been made to calculate the standard deviations of water quality from 12 am to 12 am for the last 25 h of the simulations (from hours 456 to 480) at node 11 for the uncertain parameters diameter and demand. The result shows that diameter has less impact (standard deviation 0.013 mg/L) than demand (standard deviation 0.022 mg/L). Pipe roughness alters turbulence levels and wall decay but to a lesser degree than the wall decay coefficient's direct impact. Considering one parameter uncertain at a time the standard deviation and coefficient of variation are as high as 0.015 and 0.02, respectively, excluding the pump switching periods in the MCS. The uncertainty is largest (standard deviations in the range of 0.025 mg/l) when all the parameters are considered as uncertain (Figure 4(c)).

Node 24

The temporal pattern of flow to and from the tank is shown in Figure 5(a). Water flows from the tank into the network from 6 am to 3 pm and 4 pm to 7 pm and the tank fills during the remainder of the day. Average concentration over time at node 24 is shown in Figure 5(b). From 8 am to 9 pm the average concentration is around 0.27 mg/l. During the remainder of the day the concentration level is around 0.8 mg/l. The abrupt concentration changes occur when the tank flow pattern changes. Water coming from the tank is older and has lower concentrations than flow coming directly from the source. Node 24 is located very close to the tank so the concentration responds nearly immediately to tank flow changes.

The standard deviation of node 24's chlorine concentration has peaks at 7 am, 4 pm and 9 pm resulting from variability in nodal demand and temporal demand factors (Figure 5(d)). The peaks in the standard deviation occur when demand changes cause the tank flow patterns to change. Thus, the peaks correspond to periods when tank flows are near zero (Figure 5(a)). Water quality in the tank during draining periods is lower than the water quality in the tank when flow is being supplied from the source. Thus, during the noted periods, the source and its concentration are quite different and the demand changes cause the

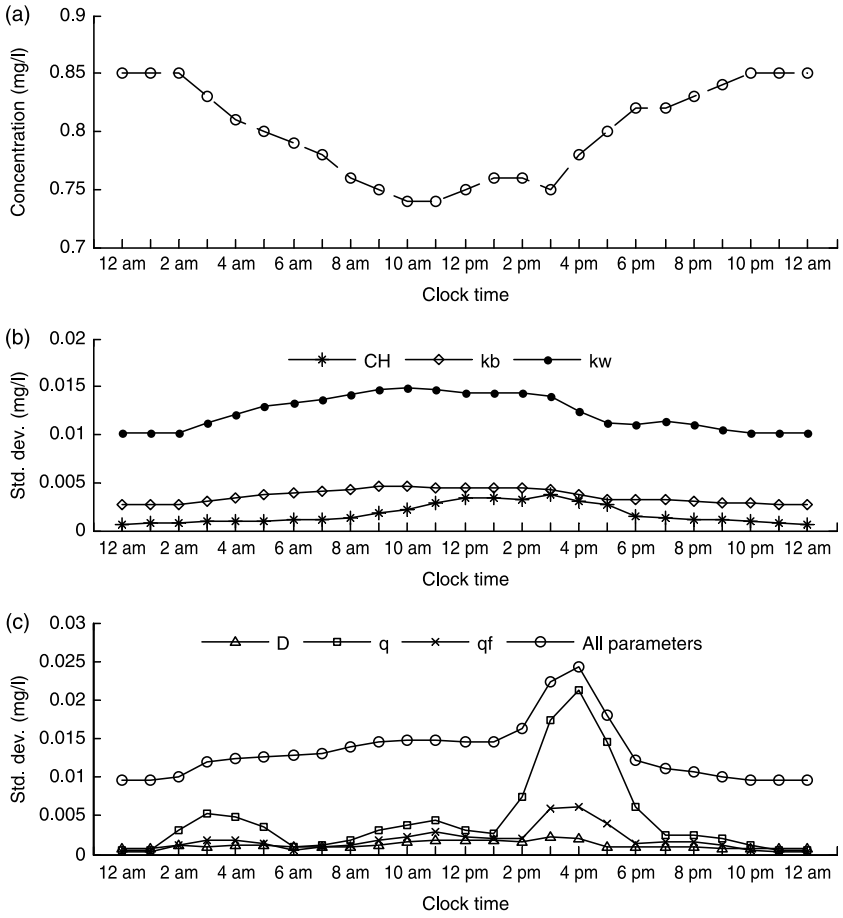

Figure 4 | (a) Temporal pattern of average concentration at node 11 (Example 1 network). (b) Temporal pattern of standard deviation of concentration at node 11 for uncertain roughness and decay coefficients under cyclical unsteady conditions (Example 1 network). (c) Temporal pattern of standard deviation of concentration at node 11 for uncertain diameter, demands, and all parameters together under cyclical unsteady conditions (Example 1 network).

source of water to change and uncertainty (standard deviation) to increase.

The relative impact of the different patterns is shown in Figures 5(c, d). The most striking result is the relative uncertainty of the output relative to individual parameters except during the flow transition periods. Except for those periods, the standard deviation of the chlorine concentration is less than 0.015 mg/l for all parameters. Thus, the coefficient of variation (CV) of the output is at most 0.04 while the input coefficients of variation were all 0.1. This result demonstrates the robustness of this system to input uncertainty during normal operations. The total effect of the set of parameters, however, can be more substantial. When all uncertain parameters are considered simultaneously, the water quality standard deviation increases in both non-transition and transition periods although the increase of standard deviation in the transition period is higher than during the non-transition period.

Focusing on individual parameters, the wall decay coefficient generally has the largest effect exclusive of the short flow reversal periods and follows a temporal pattern similar to the concentration (Figure 5(c)). Although the highest standard deviation varies, the coefficients of variation are relatively constant and near 0.02. The wall coefficient is more significant than the bulk coefficient between the hours of 10 pm and 6 am since the flow is provided by the pump station at relatively high velocities. The remainder of the parameters had very little influence on concentration uncertainty including the demand terms during the periods of well-defined flow from the tank.

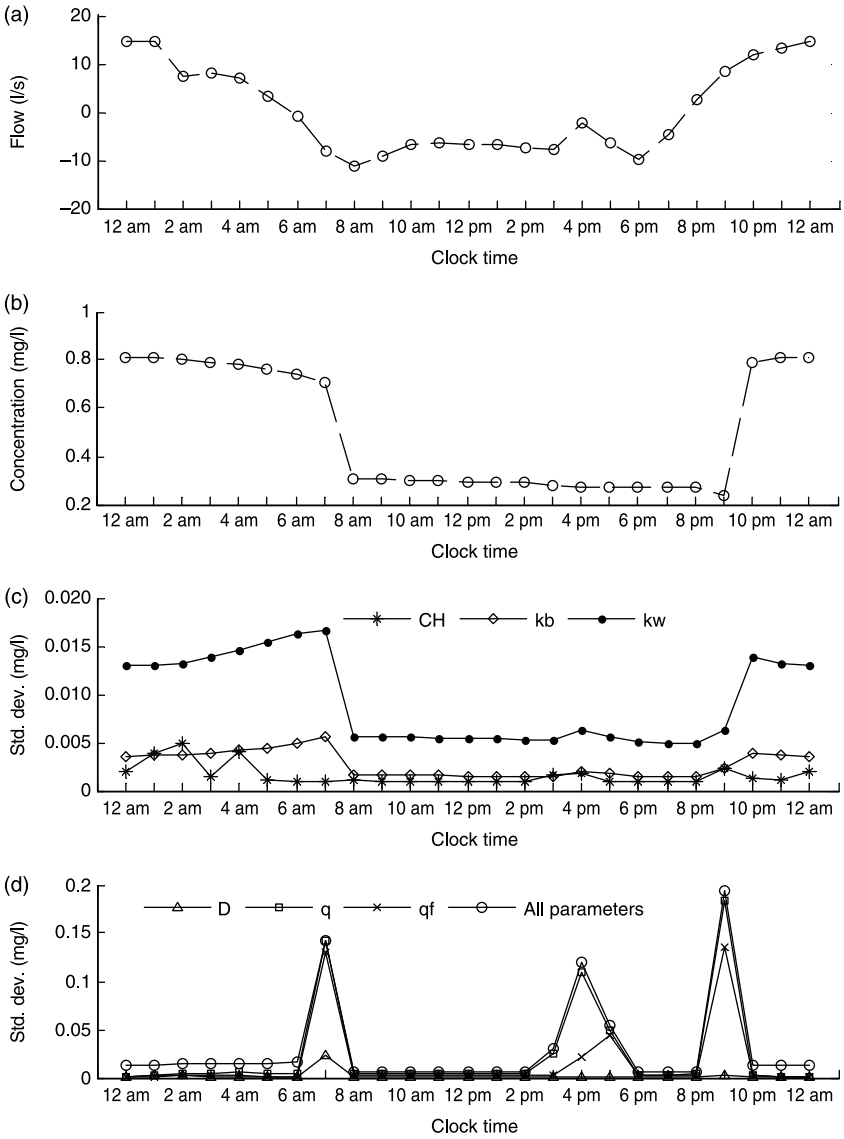

Figure 5 | (a) Temporal tank flow pattern (positive and negative values correspond to flow to and from the tank, respectively (Example 1 network). (b) Temporal pattern of average concentration at node 24 (Example 1 network). (c) Temporal pattern of standard deviation of concentration at node 24 for uncertain roughness and decay coefficients under cyclical unsteady conditions (Example 1 network). (d) Temporal pattern of standard deviation of concentration at node 24 for uncertain diameter, demands and all parameters together under cyclical unsteady conditions (Example 1 network).

The order of importance in this unsteady analysis (global wall decay coefficient, nodal demand and temporal demand factors, and bulk decay coefficient) was identical to the most significant contributors to uncertainty at node 24 for the steady state conditions (Figures 3(a, b)).

Node 26

Flow reaching node 26 has the longest travel time in the system. On average, morning water (6 am to 12 pm) supplied to node 26 is directly from the pump station with high chlorine concentrations. During the remainder of the day water reaching node 26 has been stored in the tank prior to delivery and has lower concentrations (Figure 6(a)).

Flow reaching node 26 passes through node 24. The two concentration levels at node 24 (Figure 5(b)) correspond to the tank supply (low values) and direct source supply (high values). On average, this pattern is slightly compressed when it reaches node 26 (Figure 6(a)) due to the demand

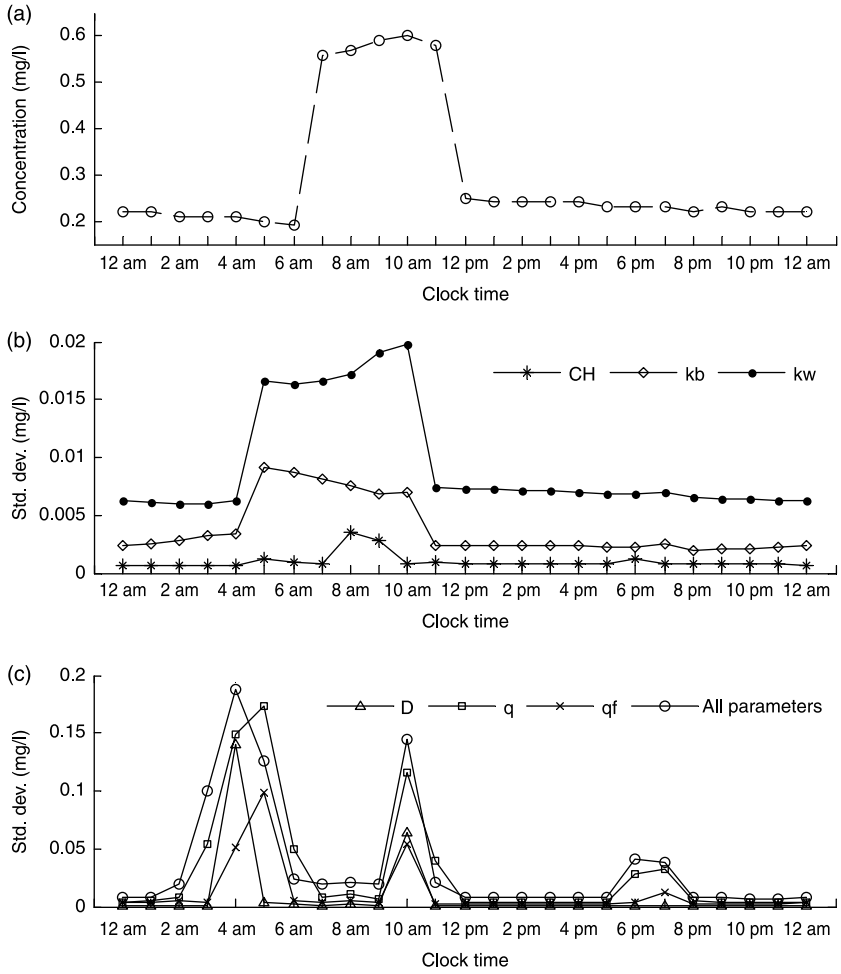

Figure 6 | (a) Temporal pattern of average concentration at node 26 (Example 1 network). (b) Temporal pattern of standard deviation of concentration at node 26 for uncertain roughness and decay coefficients under cyclical unsteady conditions (Example 1 network). (c) Temporal pattern of standard deviation of concentration at node 26 for uncertain diameter, demands, and all parameters together under cyclical unsteady conditions (Example 1 network).

variations. The 10 h elevated period at node 24 (Figure 5(b)) is reduced to 5 h due to the higher daylight hour demands (Figure 6(a)). In addition, the pattern is delayed by about 4.5 h as a result of the low velocities in pipes between nodes 24 and 26. This travel time also accounts for the lower chlorine concentrations.

The standard deviations and coefficients of variation for different individual parameters during the evening and night-time hours are as high as 0.01 and 0.04, respectively (Figures 6(b, c)). Uncertainties are elevated from about 6 am to 6 pm due to changes in hydraulic conditions and the water source (i.e. stored in a tank or supplied directly from the source) rather than changes in water quality during travel. This hypothesis was confirmed by introducing a setpoint booster at the tank outlet maintaining a constant chlorine concentration at node 24 and repeating the MCS. Uncertainty spikes were not observed in this test (not shown).

A number of interesting results are identified from Figures 6(b, c). First, the uncertainty at node 26 is consistently higher than both nodes 11 and 24 due to the larger decrease in chlorine in flow reaching that node. Second, at times the uncertainty when all parameters are considered is less than the uncertainty when a single parameter is evaluated. This result is inconsistent with the fundamental relationship in Equation (12) that shows that uncertainty should increase with additional uncertain input parameters. In this case, however, the variability in results is caused by changes in tank conditions (open/closed) which, in turn, alters the equations

that govern the system state and Equation (12) does not apply. It appears that, as more uncertain parameters are included in the analysis, the tank filling and emptying conditions are delayed and the uncertainty in output is shifted in time. Third, the nodal demand and the temporal demand factor uncertainties always had the highest impact. This factor is likely due to its direct relationship to the travel time. Next, the uncertainty peaks caused by roughness and diameter are not coincident in time. While diameters directly affect pipe velocities and travel times, pipe roughness is less direct as it alters the network flow pattern due to the head loss distribution but does not directly change the flow velocity. Finally, plotting the MCS results on normal distribution paper for all periods during the day showed that up to about the 95th percentile the model output was normally distributed (not shown).

SENSITIVITY ANALYSIS

Parameter uncertainty level

MCS runs for different input coefficients of variation (CV) for all parameters were completed to examine the relationship between the input and output uncertainty levels. The output CV for nodes 11, 24 and 26 were examined at six different times during the day. As expected, the output uncertainty increases with input uncertainty (CV) for all nodes at all times.

The output uncertainty due to global wall and bulk decay coefficients increases faster than linear as the CV is increased. Doubling the CV of k_w (from 0.05 to 0.10) increased the output standard deviation (SD) at all nodes and times by about a factor of 1.75. Doubling the CV again to 0.20 more than doubled the concentration SDs (a factor of 2.2). The change with respect to k_b was slightly more linearly proportional with increases of about 185% and 210% when the input CV was altered from 0.05 to 0.1 and 0.1 to 0.2, respectively.

Less than proportional increases in output uncertainty were observed when the total demand factor, q_j^n, uncertainty was altered. For example, when the demand CV was decreased to 50% of the base value the SD of the nodal concentration generally decreased to about 40% of its base value. Varying the demand factor uncertainty altered the supply location timing and elevated periods of high uncertainty. For most times and locations, the temporal demand factor (q_f) response was nearly linearly proportional to changes in its input uncertainty over a range of CVs from 0.05 to 0.20. Node 26 was the least consistent, particularly during periods when the source supply would change. Changes in uncertainties in pipe diameter and roughness have similar slightly less than linear proportional changes in output SDs. Node 26 was anomalous in some cases. Full display of the results can be found in Pasha (2006).

Effect of emergency storage volume

Reducing tank storage and ensuring tank turnover are means to improve water quality. Changing tank operations may also alter the uncertainty in water quality. To model tank conditions three pump control policies were developed. Each policy consists of three pumping control rules: below a minimum level turn on all three pumps, exceed a mid-tank level turn off one pump and exceed a maximum level turn off all pumps. The low emergency storage policy control rules changed pump operations at 1.5, 3.1 and 4.6 m of water in the tank, respectively. The tank levels for changing pump operations for medium and high emergency storage conditions were 3.1, 4.6 and 6.1 m and 4.6, 6.1 and 7.6 m, respectively. Medium storage is the condition evaluated in earlier sections. Note that a low emergency storage range results in a larger proportion of tank water turning over each day.

As the emergency storage increases mean concentrations decrease with longer retention times. The average daily standard deviation (excluding periods impacted by flow changes) also changes with the storage volume for all the parameters at downstream nodes (Table 4). Higher tank storage volumes increase uncertainties (standard deviations) at the downstream nodes 24 and 26 for all the parameters except the decay coefficients. Uncertainties due to the decay coefficients (both the global wall and bulk decay coefficients) decrease when tank storage volume increases (Table 4). However, since the mean concentrations decrease with higher storage, the relative uncertainty as represented by the coefficient of variation (CV) increases as a result of uncertainty in the decay coefficients. Variation in the uncertainties at nodes where the tank does

Table 4 | Average standard deviation (mg/l) for different tank storage volumes under unsteady conditions (Example 1 network)

Node	Conditions	Diameter	Roughness	Demand	Bulk decay	Global wall decay	Demand factor	All parameters
26	High storage	0.0039	0.0019	0.0194	0.0056	0.0123	0.0100	0.0258
	Medium storage	0.0049	0.0015	0.0175	0.0056	0.0143	0.0081	0.0247
	Low storage	0.0029	0.0018	0.0153	0.0063	0.0139	0.0077	0.0240
24	High storage	0.0028	0.0045	0.0137	0.0038	0.0107	0.0088	0.0208
	Medium storage	0.0017	0.0022	0.0122	0.0036	0.0124	0.0072	0.0199
	Low storage	0.0017	0.0032	0.0103	0.0040	0.0117	0.0064	0.0181
11	High storage	0.0012	0.0017	0.0047	0.0038	0.0111	0.0019	0.0130
	Medium storage	0.0012	0.0017	0.0046	0.0036	0.0123	0.0019	0.0134
	Low storage	0.0013	0.0018	0.0045	0.0038	0.0111	0.0018	0.0136

not provide water (or the tank provides water for a shorter time) is negligible (e.g. node 11). Thus, for this system, reducing emergency storage improves system water quality and makes system conditions more stable and less uncertain.

Effect of demand pattern

Since demand factors had the largest influence on the output uncertainty, MCS runs were completed for three other demand patterns. The magnitude of the total demand was increased and decreased by 10% in patterns 1 and 2, respectively. The third pattern increased the demand at all times by 10% except at 8 am and 6 pm when the peaks are increased by 25% representing a more summer-like condition. Compared to the original demand pattern, the magnitude of the output uncertainties did not change for any of the three new patterns.

While the temporal pattern of standard deviations for node 11 did not change, the time distribution of standard deviations of chlorine concentration for nodes 24 and 26 were altered (Figure 7). Since the temporal demand patterns had similar shapes as for the base condition, the timing of demand and temporal demand factors uncertainties were unchanged. However, the peaks associated with pipe roughness and diameter were shifted in time. Like the base condition, these peaks are caused by changes in water source. A new peak was added for the third pattern due to variability in water source in the early evening. Overall, the similar uncertainty magnitude shows the relative stability of water quality in this water distribution system.

APPLICATION NETWORK: EXAMPLE 2

The second network analyzed is a real network that consists of 90 nodes, 116 pipes, 1 source, 1 tank, and 4 pumps connected to the source. The tank is considered only in unsteady conditions. The hydraulic time step, quality time step and pattern time step were 1:00, 0:05 and 1:00 h, respectively. Chlorine is the disinfectant with an input concentration of 1.25 mg/l assuming a first-order reaction with $k_b = -0.3$ 1/d and $k_w = -0.4$ 1/d. Of a total of 90 nodes, 40 nodes have zero demand. 0.879 m^3/s (31.05 cfs or 3,166 m^3/h) is the average total system demand. Node 79 is the furthest node from the source and thus has the longest water age of about 26 h with the lowest concentration. The nodal concentrations were examined at three locations in the system (nodes, 19, 52 and 79 (Figure 8)).

Similar to Example 1 diameter is considered uniformly distributed with a maximum variation of 12.7 mm (0.5 inches) and other parameters are considered normally distributed while roughness and demand are assumed to follow a truncated normal distribution. In steady state analysis, the demand is constant and the simulation was performed for 90 h to ensure steady conditions for all locations. The last hour's concentrations were evaluated. In unsteady analysis the 24 h demand pattern was repeated for the 240 h simulation to ensure cyclical steady conditions. The last 24 hours concentrations were evaluated.

Similar to the Example 1 network, 10,000 realizations were conducted in each experiment to ensure convergence. A set of experiments was completed with only one parameter being uncertain while the others are constant.

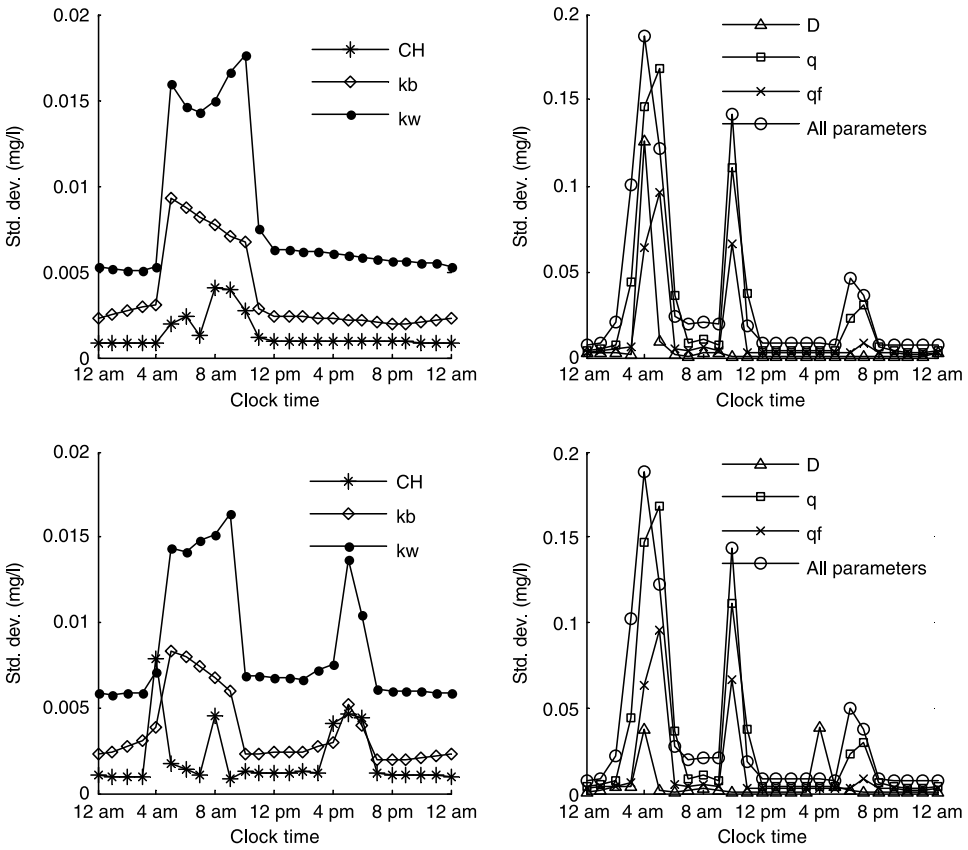

Figure 7 | Temporal pattern of standard deviation of concentration for different uncertain parameters at node 26 under cyclical unsteady conditions for demand pattern 2 (top row) and 3 (bottom row) for Example 1 network.

These experiment results were compared with an experiment with all parameters considered uncertain.

Steady conditions

Box and whisker plots are shown for steady state experiments in Figure 9. Similar to the Example 1 network, the important parameters are global wall decay coefficient, bulk decay coefficient and demand. As expected, when all the parameters are considered uncertain together the output uncertainty level becomes the highest. Separately, the global wall decay coefficient has the highest impact at node 52 which is close to the pump station. While demand has a small impact at node 52, it has higher impacts at nodes 19 and 79. The bulk decay coefficient shows similar observations as found in Example 1. It has higher impact where the water age is higher or the water turbulence is less (node 79) but relatively smaller impacts where water age is less or the turbulence is higher (nodes 19 and 52). Similar to the Example 1 network, diameter and pipe roughness have small contributions to overall uncertainty.

Unsteady conditions

Unsteady condition results are shown in Figures 10–12. Observations that are similar to Example 1 can be made for this network. Uncertainty spikes are observed due to either change in pump schedule or change in flow direction to the tank. Node 19 is relatively close to the pump station and is not affected by the tank flow (Figure 10). The uncertainty spikes at this node are observed due to changes in the pump operation. However, node 52 is located close to the tank and is directly affected by the tank flow. Uncertainty spikes at this node are observed when the tank flow direction changes (Figures 11(a, b)). Node 79 is the distant node and the tank effect is relatively small. As a result, the

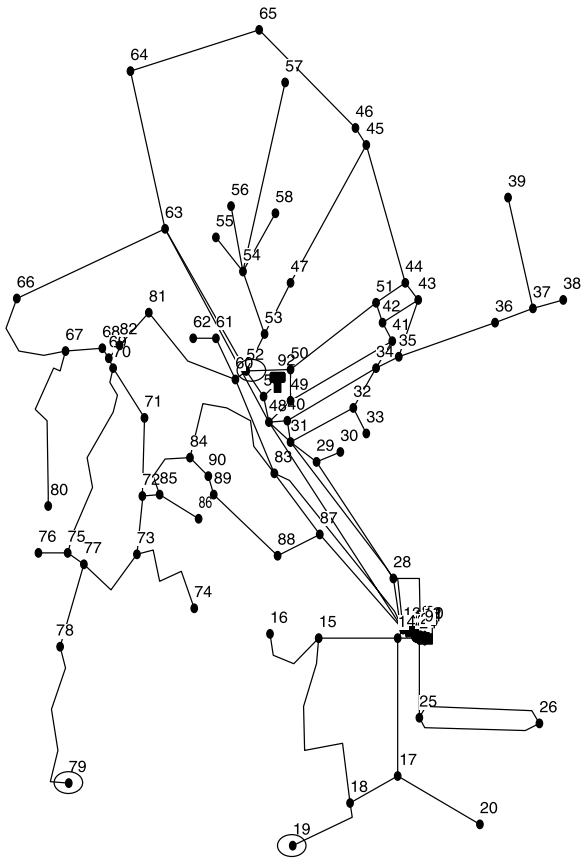

Figure 8 | Example 2 network.

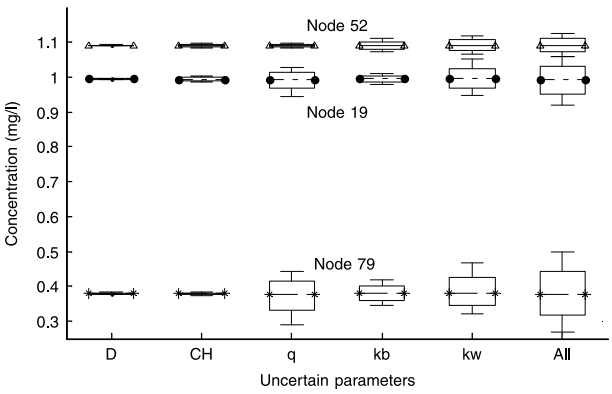

Figure 9 | Box and whisker diagrams for MCS results under steady conditions for individual parameter uncertainty (Example 2 network).

spikes are not significant (Figure 12). The global wall decay coefficient has the highest impact on uncertainties for nodes 19 and 52 while the nodal demand has the highest impact at node 79.

DISCUSSION

The most salient result from this analysis is the relatively small uncertainty in water quality as a result of the model input uncertainty during much of the day at most locations. Changes in supply result in significant uncertainty but parameter uncertainties do not have a tremendous impact on model output. For a system operator or administrator, this result is promising. If the model is generally robust under normal operations, the delivered water quality is likely maintained under those conditions. As systems move to optimizing operations to maintain water quality, an MCS analysis such as this would be useful to ensure standards will be met.

In addition, the limited uncertainty is promising for the detection of contaminant intrusions. Contamination events are detected as deviations from average conditions. Since water quality is relatively stable, excursions from those conditions are likely indicative of an outside influence and relatively small changes can be identified. During mixed supply periods, confidence levels would have to be increased or additional logic could be incorporated to provide information on the system operations (i.e. the tank empty/fill condition).

Although stable model results are useful for some purposes, they pose difficulties in water quality model calibration and potential predictions under extreme conditions. A water quality model requires two sets of model parameters: hydraulic and water quality. Hydraulic parameters include pipe diameters and roughnesses, and nodal demands. Distributed demands are difficult to ascertain and are typically generated from experience and judgment. Pipe parameters can be estimated and improved from pressure test data. These inputs in a hydraulic simulation give water velocities and travel times that drive water quality. All of these parameters can be improved with tracer tests that measure travel times. Tracer tests, however, are strongly influenced by the actual demands occurring during the test. In the small system examined here, the demand influence on water quality is not significant but this may not translate to water age and travel time. It was more significant in the large system but only at the distal nodes.

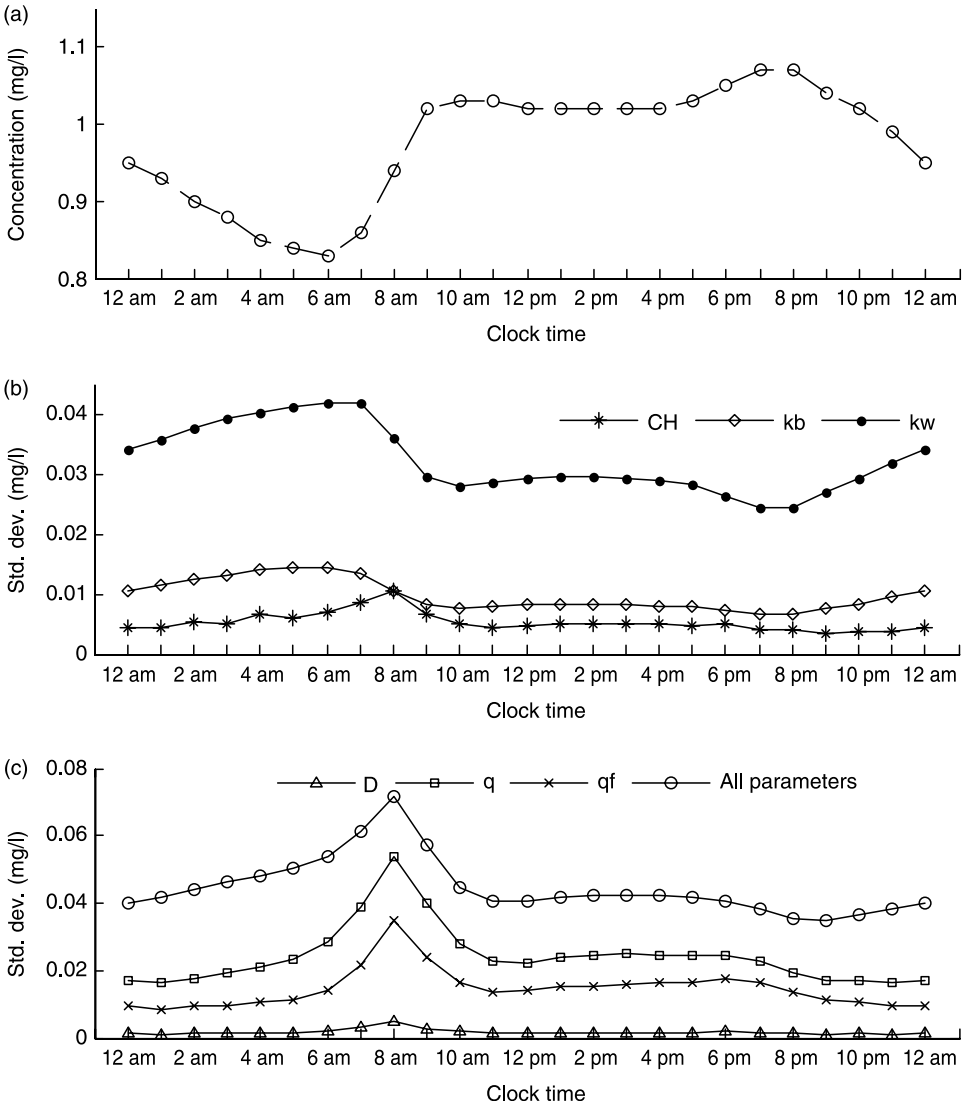

Figure 10 | (a) Temporal pattern of average concentration at node 19 (Example 2 network). (b) Temporal pattern of standard deviation of concentration at node 19 for uncertain roughness and decay coefficients under cyclical unsteady conditions (Example 2 network). (c) Temporal pattern of standard deviation of concentration at node 19 for uncertain diameter, demands, and all parameters together under cyclical unsteady conditions (Example 2 network).

Bulk decay coefficients can be determined off-line in jar tests. However, wall decay coefficients must be calibrated with field data. The relatively limited uncertainty of water quality to model parameters presents a difficult problem. It suggests that a reasonable range of parameter values (wall decay and others) will provide similar water quality estimates. Thus, calibration for the wall decay parameter from field disinfectant measurements under average conditions will likely not provide its unique value. This is acceptable for normal operations but may not be so for extreme conditions or during studies to modify operations. An inability to identify the true parameter value is particularly difficult in more complex water quality models that require multiple parameters to describe water quality transformations in a pipe. Another use of water quality models is to examine water quality under new operational conditions or extreme conditions such as pipe breaks and pump failures. These conditions have been examined here to a very limited extent with promising conclusions but deserve study in a similar vein.

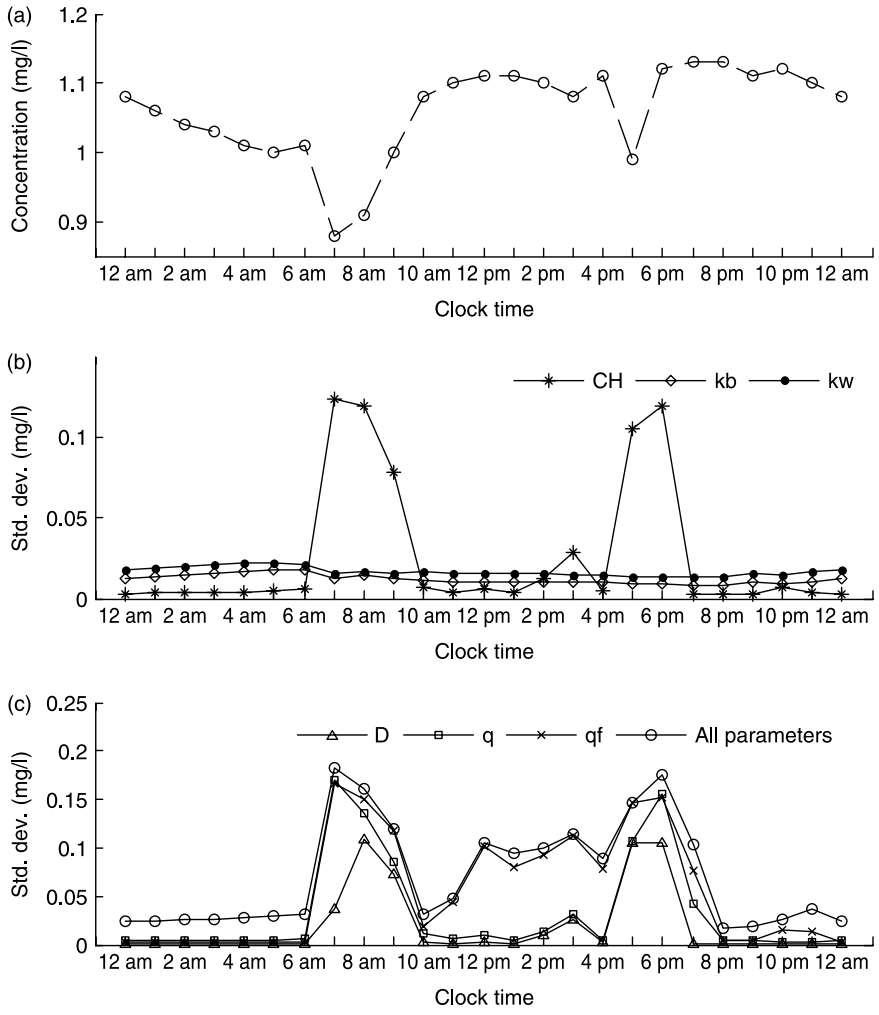

Figure 11 | (a) Temporal pattern of average concentration at node 52 (Example 2 network). (b) Temporal pattern of standard deviation of concentration at node 52 for uncertain roughness and decay coefficients under cyclical unsteady conditions (Example 2 network). (c) Temporal pattern of standard deviation of concentration at node 52 for uncertain diameter, demands, and all parameters together under cyclical unsteady conditions (Example 2 network).

Tracer tests with simultaneous water quality measurements are the best practical method for ascertaining in-system water quality parameters but demand estimates remain an issue. Given that these tests are usually completed under normal operations and the sensitivity to wall decay is not very significant, a wall decay estimate from a tracer study result is likely to be not very robust. During hydraulic calibration, extreme conditions are introduced through a hydrant test. No analogous long-term stress test has been proposed for water quality parameter estimation. Research is in this direction appears necessary.

To summarize, based on the MCS results, if a model is calibrated for normally occurring conditions, model calibration will likely result in in-system parameters that are not robust. However, when modeling those typical conditions, this paper shows that the range of model outputs based on those parameters will not be wide (except for changes resulting in system dynamics (tank/source operations)). However, the impact of less common conditions is unclear beyond some simple tests. More study is needed on looped systems, failure conditions, growth changes and alternative system operations that intend to minimize pumping costs or disinfection injections (possibly in conjunction with valving).

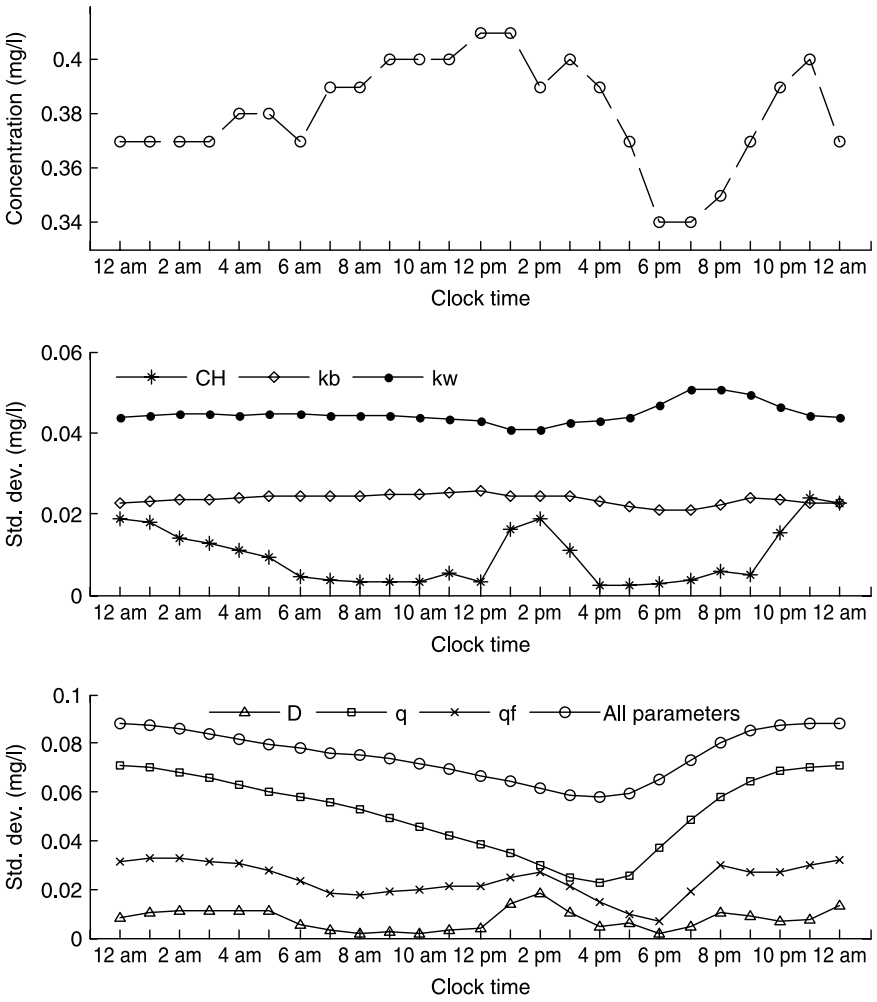

Figure 12 | (a) Temporal pattern of average concentration at node 79 (Example 2 network). (b) Temporal pattern of standard deviation of concentration at node 79 for uncertain roughness and decay coefficients under cyclical unsteady conditions (Example 2 network). (c) Temporal pattern of standard deviation of concentration at node 79 for uncertain diameter, demands, and all parameters together under cyclical unsteady conditions (Example 2 network).

CONCLUSIONS

MCS was applied to two water distribution systems to study the effect of uncertain parameters on water quality predictions. Steady and unsteady conditions were analyzed for the input parameters' coefficient of variation of 0.1. The parameters considered are the bulk and global wall decay coefficients, pipe roughnesses and diameters, and nodal demands for steady conditions. For unsteady analysis, a temporal demand factor is added. The effect of parameter uncertainty is examined by varying one parameter with others remaining fixed in both steady and unsteady cases. To further examine the relative effect of a parameter under steady conditions, each parameter was fixed while all parameters were considered as uncertain.

Four primary conclusions were drawn from the results. First, the relative impact for these two systems due to the uncertain input was small. Second, from the steady and unsteady analyses the influence of decay coefficients tended to be the largest of all parameters. Changes in flow conditions caused by demand uncertainty caused elevated uncertainty levels but during the consistent flow conditions the effect of demand uncertainty was low. Third, the relative magnitude of the standard deviation of the model output was directly related to the distance from the source (under consistent flow conditions). Finally, for the systems considered and the

assumption of uncorrelated parameters, the impact of uncertainties were not additive in the unsteady case and, in some cases, the output standard deviation for all uncertain parameters together was less than the uncertainty for a single uncertain parameter due to the lagging effect of uncertainties caused by changing the flow pattern in the system.

A series of sensitivity analyses were completed for the Example 1 network and the following conclusions were reached. Although it promotes chlorine decay, as emergency storage was increased the relative uncertainty increased at downstream nodes. The rate of change of the output uncertainty was constant or increased with increasing parameter uncertainty levels. The impact of altering the demand pattern over the range considered was small.

The implications of uncertainties on modeling water quality are significant in terms of calibration and model application. Determining a set of parameters that provide a match with field measurements is likely not very difficult as many parameter sets will provide similar results. However, gaining confidence in a calibration may prove difficult due to the limited uncertainty of the water quality under normal operational conditions. Reasonable parameters appear to be relatively robust for normal operations but more extreme results may not be accurately predicted. To begin to further assess these issues, additional uncertainty analyses should be completed considering spatial and temporal correlations between demands, for travel time conditions and for highly stressed systems or under failure conditions. This study was conducted with an emphasis on the state-of-the-art in water distribution system modeling under normal operating conditions. Pressure-driven demand modeling (Giustolisi *et al.* 2008) should be considered in a similar framework to determine the impact of these conditions on model prediction uncertainties.

ACKNOWLEDGEMENTS

The authors thank Steven Buchberger and Nabin Khanal for providing the all-pipe Net2A network. We also appreciate all reviewers of this work and their input to improve the presentation and quality of the work.

REFERENCES

Abramowitz, M. & Stegun, I. A. 1972 *Handbook of Mathematical Functions*. Dover Press, New York.

Bao, Y. & Mays, L. W. 1990 Model for water distribution system reliability. *J. Hydraul. Eng. ASCE* **116** (9), 1119–1137.

Barkdoll, B. D. & Didigam, H. 2004 Effect of user demand on water quality and hydraulics of distribution systems. In *Proceedings of the ASCE World Water and Environmental Resources Congress, Salt Lake City, UT, 27 June–1 July* (ed. P. Bizier & P. DeBarry). ASCE, New York.

Boulos, P. F., Lansey, K. E. & Karney, B. W. 2004 *Comprehensive Water Distribution Systems Analysis Handbook for Engineers and Planners*, pp. 3/12–13. MWH Soft, Inc, Pasadena, CA, 5/8–9, 6/3–5, 6/16–18.

Giustolisi, O., Savic, D. A. & Kapelan, Z. 2008 Pressure-driven demand and leakage simulation for water distribution networks. *J. Hydraul. Eng. ASCE* **134** (5), 626–635.

Khanal, N., Steven, G., Buchberger, S. G. & McKenna, S. A. 2006 Distribution system contamination events: exposure, influence, and sensitivity. *J. Water Resour. Plann. Manage.* **132** (4), 283–292.

Pasha, M. F. K. 2006 *Uncertainty Analysis and Calibration of Water Distribution Quality Models*. Dissertation submitted in partial fulfillment of the PhD requirements, Department of Civil Engineering and Engineering Mechanics, University of Arizona.

Pasha, M. F. K. & Lansey, K. E. 2005 Analysis of uncertainty on water distribution hydraulics and water quality. In *Proceedings of the ASCE World Water and Environmental Resources Congress, Anchorage, AK, 15–19 May* (ed. R. Walton). ASCE, New York, doi: 10.1061/40792(173)1.

Rossman, L. A. 2002 *EPANET User's Manual*. Environmental Protection Agency, Cincinnati, OH.

Rossman, L. A., Clark, R. M. & Grayman, W. M. 1994 Modeling chlorine residuals in drinking-water distribution systems. *J. Environ. Eng.* **120** (4), 803–820.

Sadiq, R., Kleiner, Y. & Rajani, B. 2004 Aggregative risk analysis for water quality failure in distribution networks. *J. Water Supply Res. Technol. Aqua* **53** (4), 241–261.

Todini, E. & Pilati, S. 1988 A gradient algorithm for the analysis of pipe networks. In *Computer Applications in Water Supply, System Analysis and Simulation* (ed. B. Coulbeck & C. H. Orr), **Vol. 1**, pp. 1–20. John Wiley & Sons, Chichester.

Tung, Y. K. & Yen, B. C. 2005 *Hydrosystems Engineering Uncertainty Analysis*, pp. 6/254–262. McGraw-Hill, New York.

Wagner, J. M., Shamir, U. & Marks, D. H. 1988 Water distribution reliability: simulation methods. *J. Water Resour. Plann. Manage.* **114** (3), 276–294.

Xu, C. & Goulter, I. 1998 Probabilistic model for water distribution reliability. *J. Water Resour. Plann. Manage.* **124** (4), 218–228.

First received 23 June 2008; accepted in revised form 4 December 2008. Available online September 2009